

Vapor–Liquid Equilibrium Study of an Absorption Heat Transformer Working Fluid of (HFC-32 + DMF)

Xiao Hong Han, Ying Jie Xu, Zan Jun Gao, Qin Wang,* and Guang Ming Chen

Institute of Cryogenics and Refrigeration, Zhejiang University, Hangzhou 310027, China

ABSTRACT: The absorption heat transformer (AHT) is an important energy-saving device that can be driven by low-grade energy. In this work, the mixture of difluoromethane (HFC-32) and *N,N*-dimethylformamide (DMF) is considered as a promising new working fluid for AHTs. Vapor–liquid equilibrium data for (HFC-32 + DMF) were measured over the temperature range from (283.15 to 363.15) K using an equilibrium apparatus with continuous vapor-phase circulation. Throughout the overall experiment, there was no stratification or sediment generation, and the color of the liquid in the equilibrium cell was the same before and after the experiment. The above-mentioned results suggest that any ratio of HFC-32 and DMF could be miscible. The experimental data were correlated using the NRTL model. The average relative deviation of the pressure was 1.65 %, and the maximum relative deviation of the pressure was 4.24 %. The calculated results showed good agreement with the experimental data. It is shown that the mixture exhibits a negative deviation from Raoult's law.

INTRODUCTION

Under the background of the global energy crisis, the utilization of low-grade energy is more and more important for the world. Because absorption heat transformers (AHTs) can use waste heat economically, thereby decreasing the consumption of primary energy and minimizing the negative impact on the environment, AHT technology is being developed rapidly.¹ In an AHT, the selection of working pairs is important for various applications. For example, new working fluids can extend the operating range to higher temperatures in the use of absorption heat pumps.

At present, the most common working pairs are ammonia + water and water + lithium bromide, but the applications of these two types of working pairs are limited by their own shortcomings, such as the need for extra apparatus for distillation, the occurrence of crystallization, pressures lower than atmospheric pressure, and refrigeration temperatures that cannot be below 0 °C. Therefore, many researchers have paid a great deal of attention to the development of new refrigerant–absorbent pairs.^{2–7} Among these, fluorocarbon-based refrigerants, together with suitable nonvolatile organic solvents such as dimethyl ether of tetraethylene glycol (DMETEG), dibutyl phthalate (DBPh), and *N,N*-dimethylformamide (DMF) appear to be promising. In comparison with DMETEG and DBPh, DMF has several advantages, such as considerably lower price, significantly lower viscosity, and higher absorption capacity for fluorocarbon-based refrigerants (in an absorption refrigeration system, the absorbent should have a strong ability to absorb the refrigerant).⁸

Literature reviews indicated that HCFC-22 is the best fluorocarbon refrigerant for use in absorption refrigeration systems.^{8–10} However, because of regulations to phase out chlorofluorocarbons (CFCs) and hydrochlorofluorocarbons (HCFCs), hydrofluorocarbons (HFCs) and mixtures of these fluids are being investigated as alternative refrigerants.^{11–14}

Difluoromethane (HFC-32), which has superior environmental performance [ozone-depletion potential (ODP) = 0, global-warming potential (GWP) = 675¹⁵] and favorable thermophysical, equilibrium, and transport properties, is an attractive long-term candidate to replace

HCFC-22. For example, it can be used alone in vapor-compression refrigeration systems.¹⁶ In addition, some mixed refrigerants containing HFC-32 are being studied by some researchers.^{17–20} HFC-32 also can be used as a substitute for chlorofluorocarbons in absorption heat pumps and refrigeration units. Thus, DMF (absorbent) and HFC-32 (refrigerant) seem to be one of the most promising combinations for use in absorption refrigeration systems. In order to evaluate the performance of absorption heat pumps and refrigeration units using the mixture (DMF + HFC-32), accurate knowledge of vapor–liquid equilibrium data for the working pair is necessary. In this work, reliable p – T – x data for (HFC-32 + DMF) were measured from $T = (283.15 \text{ to } 363.15) \text{ K}$ over the complete range of compositions using an equilibrium apparatus with continuous vapor-phase circulation. The experimental data were correlated using the nonrandom two-liquid (NRTL) model.²¹ The solubility data for HFC-32 were used to determine the activity and activity coefficient of HFC-32 in the refrigerant–absorbent solutions. The effects of DMF on the solubility of HFC-32 and the properties of the solutions are discussed.

EXPERIMENTAL SECTION

Chemicals. HFC-32 was provided by Zhejiang Lantian Environmental Protection Co., Ltd. (FLTCO) and had a mass fraction purity of > 99.9 %. DMF was supplied by SamSung Fine Chemical Co. Ltd. (Korea) and had a mass fraction purity of > 99.99 %. Both samples were used without any further purification.

Apparatus. The solubility of HFC-32 in DMF at various temperatures and pressures was measured using an equilibrium apparatus with continuous vapor-phase circulation. Details of the apparatus have been described by Han and co-workers.^{20,22} The apparatus consists mainly of an equilibrium cell, a water bath, a

Special Issue: John M. Prausnitz Festschrift

Received: October 29, 2010

Accepted: January 24, 2011

Published: February 14, 2011

pressure transducer, a platinum temperature sensor, temperature and pressure controllers, and a motorized blender.

The equilibrium cell could be maintained within ± 0.01 K for experimental temperatures between (283.15 and 363.15) K by means of highly accurate temperature control equipment (Sr253-2I-N-0060010, Shimaden, Japan). The temperature in the equilibrium cell was monitored by using a four-lead 25Ω platinum resistance thermometer (Yunnan Instrument, WZPB-2). The overall temperature uncertainty for the measurement system was less than ± 15 mK. The equilibrium pressure was measured using a pressure transducer (Druck PMP 4010), a differential-pressure null transducer (Xi'an Instrument, 1151DP), an oil-piston-type dead-weight pressure gauge (Xi'an Instrument, YS-60), and an atmospheric pressure gauge (Ningbo Instrument, DYM-1). A sensitive differential-pressure null transducer separated the sample from the oil-piston-type dead-weight pressure gauge. The whole pressure measurement system had an uncertainty of ± 1.6 kPa.

In this work, the mass of the mixture (refrigerant + DMF) was determined by weighing the DMF and refrigerant on an electronic scale [Sartorius Scientific Instruments (Beijing) Co., Ltd., BS4000S] with an uncertainty of 0.01 g. The mass fraction of refrigerant in the liquid phase (w_R) is given by

$$w_R = \frac{m_R - m_{V,R}}{m_R + m_{DMF} - m_{V,R}} \quad (1)$$

where m_{DMF} is the mass of DMF, m_R is the additive refrigerant mass, and $m_{V,R}$ is the vapor-phase refrigerant mass. The masses m_{DMF} and m_R were determined on the electronic scale. The mass of refrigerant in the vapor phase was obtained using the following equation:

$$m_{V,R} = \rho V \quad (2)$$

where ρ is the refrigerant density in the vapor phase, as obtained using REFPROP,²³ and the vapor-phase refrigerant volume V consists of two parts, the stainless steel pipe volume (V_1) and the upper vapor space volume in the equilibrium cell (V_2). In this work, by measurement, the vapor measurement uncertainty in the total volume was ± 1.15 cm³. The total uncertainty in the liquid-phase mole fraction of the refrigerant (x_R) was within ± 0.002 .

Experimental Procedures. In each experiment, the system was preflushed with alcohol and then dried under vacuum at room temperature for 30 min, after which the system was purged with HFC-32 to remove the last traces of DMF. The above procedure was repeated two or three times to ensure that the last traces of DMF had been removed.

The system was first evacuated, and then the equilibrium cell was filled with a specified mass of DMF. Next, the system was cooled to near 275 K, and the equilibrium cell was then filled with the desired amount of HFC-32. After the equilibrium cell was filled, the thermostat bath temperature was controlled at the experimental temperature. It was believed that 2 h or more was sufficient to establish a thermal equilibrium state between the cell and the thermostat bath. At low temperatures and high concentrations of DMF, a longer time was required for equilibrium to be reached. After the equilibrium was established, the data (temperature, pressure, and mass fraction of HFC-32 in liquid phase) were recorded.

RESULTS AND DISCUSSION

P - T - x data were measured for the binary system (HFC-32 + DMF) from $T = (283.15$ to $363.15)$ K, and the results are shown in Table 1. Throughout the work, x indicates the liquid-phase mole fraction and p the pressure in kPa.

Throughout the overall experiment, there was no stratification or sediment generation, and the color of the liquid in the equilibrium cell was the same before and after the experiment. The above-mentioned results suggest that any ratio of HFC-32 and DMF could be miscible. In addition, the vapor phase of the binary mixture (HFC-32 + DMF) was analyzed using a gas chromatograph (GC) equipped with a flame ionization detector (FID) (model GC112A, China), where it was held at a constant temperature of 343.15 K for 4 days. The GC was calibrated with pure components of known purity and with mixtures of known composition that were prepared gravimetrically. The results showed the HFC-32 had no change over time, suggesting that no chemical reactions occurred. Moreover, the analysis showed that there was almost no DMF in the vapor phase of the mixture.

In this work, the experimental data were correlated using the NRTL model for a binary system, which can be described as follows:

$$\ln \gamma_1 = x_2^2 \left[\frac{\tau_{21} G_{21}^2}{(x_1 + x_2 G_{21})^2} + \frac{\tau_{12} G_{12}}{(x_2 + x_1 G_{12})^2} \right] \quad (3)$$

where γ_1 is the activity coefficient of component 1, x_1 and x_2 are the mole fractions of the components, and G_{12} and G_{21} are defined as

$$G_{12} = \exp(-\alpha \tau_{12}) \quad (4)$$

and

$$G_{21} = \exp(-\alpha \tau_{21}) \quad (5)$$

In eqs 3 to 5, α , τ_{12} and τ_{21} are the binary equation parameters. In order to consider the temperature dependence of the parameters τ_{12} and τ_{21} in the NRTL model, the following formulas, each containing two parameters, were adopted for correlation

$$\tau_{12} = \frac{\tau_{12}^{(0)} + \tau_{12}^{(1)} \ln(T)}{RT} \quad (6)$$

$$\tau_{21} = \frac{\tau_{21}^{(0)} + \tau_{21}^{(1)} \ln(T)}{RT} \quad (7)$$

in which R is the gas constant. Values of the parameters α , $\tau_{12}^{(0)}$, $\tau_{12}^{(1)}$, $\tau_{21}^{(0)}$, and $\tau_{21}^{(1)}$ in the NRTL equation were obtained by minimizing the following objective function (OBF) using the experimental vapor pressure data:

$$\text{OBF} = \sum_{i=1}^N (\ln \gamma_{1,\text{cal}} - \ln \gamma_{1,\text{exp}})_i^2 \quad (8)$$

where N is the number of experimental points, $\gamma_{1,\text{exp}}$ is the experimental activity coefficient, and $\gamma_{1,\text{cal}}$ is the calculated activity coefficient.

For the mixture (HFC-32 + DMF), the vapor phase is composed of only HFC-32 vapor because of the negligible volatility of DMF, so the vapor-liquid equilibrium can be obtained using eq 9:

$$p = \gamma_1 x_1 p_1^s \exp \left[\frac{V_1^L (p - p_1^s)}{RT} \right] \quad (9)$$

where p and T are the vapor pressure and temperature of the mixture, respectively, p_1^s is the vapor pressure of the pure refrigerant, V_1^L is the molar volume of the saturated liquid at T ,

Table 1. Vapor Pressure Data for (HFC-32 (1) + DMF (2)) Mixtures

T/K	x_1	$p_{\text{exp}}/\text{kPa}$	$p_{\text{cal}}/\text{kPa}$	$\delta p/\%^a$
283.15	0.1265	124.33	123.32	0.82
	0.2604	253.48	259.91	2.54
	0.3616	358.30	367.60	2.59
	0.4832	487.51	502.51	3.08
	0.5886	622.34	624.54	0.35
	0.6412	689.61	687.06	0.37
	0.7176	790.83	779.54	1.43
	0.7470	820.04	815.49	0.56
	0.8116	902.22	894.84	0.82
	0.8603	953.38	954.38	0.10
293.15	0.9657	1074.50	1076.17	0.16
	0.1251	158.61	153.05	3.51
	0.2616	319.03	328.62	3.00
	0.3620	451.72	465.08	2.96
	0.4859	629.86	643.45	2.16
	0.5856	801.65	796.46	0.65
	0.6404	905.02	884.42	2.28
	0.7164	1015.99	1011.23	0.47
	0.7458	1072.41	1061.62	1.01
	0.8112	1180.58	1175.68	0.42
303.15	0.8600	1251.31	1261.08	0.78
	0.9656	1425.99	1431.35	0.38
	0.1244	192.74	188.91	1.99
	0.2563	388.47	399.45	2.83
	0.3632	562.43	579.97	3.12
	0.4875	796.69	804.80	1.02
	0.5845	1005.84	994.52	1.13
	0.6434	1150.56	1117.18	2.90
	0.7221	1322.21	1290.96	2.36
	0.7495	1379.40	1354.31	1.82
313.15	0.8107	1513.53	1500.22	0.88
	0.8596	1604.50	1619.55	0.94
	0.9655	1855.41	1862.77	0.40
	0.1234	231.32	230.62	0.30
	0.2547	484.26	487.13	0.59
	0.3606	685.28	705.33	2.93
	0.4833	976.87	975.82	0.11
	0.5806	1239.73	1208.65	2.51
	0.6385	1411.53	1357.64	3.82
	0.7186	1623.17	1579.36	2.70
323.15	0.7473	1704.82	1664.00	2.39
	0.8088	1862.57	1855.79	0.36
	0.8582	1995.23	2019.50	1.22
	0.9652	2347.44	2379.81	1.38
	0.1217	285.55	277.05	2.98
	0.2521	585.93	584.36	0.27
	0.3580	822.30	845.51	2.82
	0.4813	1166.93	1168.34	0.12
	0.5789	1482.84	1445.77	2.50
	0.6380	1677.75	1627.30	3.01
333.15	0.7176	1917.24	1894.24	1.20
	0.7444	2004.47	1991.58	0.64
	0.8085	2229.34	2244.52	0.68
	0.8576			
	0.9650			
	0.1196			
343.15	0.2511			
	0.3572			
	0.4806			
	0.5781			
	0.6333			
	0.7112			
	0.7391			
	0.7984			
	0.8522			
	0.1181			
353.15	0.2499			
	0.3561			
	0.4797			
	0.5773			
	0.6326			
	0.7109			
	0.7388			
	0.7931			
	0.8470			
	0.1164			
363.15	0.2493			
	0.3555			
	0.4792			
	0.5770			
	0.6323			
	0.7102			
	0.7376			
	0.1144			
	0.2484			
	0.3548			
373.15	0.4776			
	0.5765			
	0.8576			
	0.9650			

Table 1. Continued

T/K	x_1	$p_{\text{exp}}/\text{kPa}$	$p_{\text{cal}}/\text{kPa}$	$\delta p/\%^a$
333.15	0.8576	2425.77	2460.61	1.44
	0.9650	2924.54	2994.12	2.38
	0.1196	331.41	326.13	1.59
	0.2511	708.44	693.61	2.09
	0.3572	991.51	1000.49	0.91
	0.4806	1392.93	1377.34	1.12
	0.5781	1736.95	1700.23	2.11
	0.6333	1908.18	1898.35	0.52
	0.7112	2182.56	2206.80	1.11
	0.7391	2281.00	2328.19	2.07
343.15	0.7984	2515.19	2614.77	3.96
	0.8522	2798.85	2917.52	4.24
	0.1181	382.44	376.91	1.45
	0.2499	804.87	804.42	0.06
	0.3561	1141.96	1159.82	1.56
	0.4797	1598.84	1596.35	0.16
	0.5773	1982.35	1972.29	0.51
	0.6326	2201.78	2204.93	0.14
	0.7109	2567.28	2573.26	0.23
	0.7388	2698.64	2719.81	0.78
353.15	0.7931	2986.93	3039.09	1.75
	0.8470	3294.41	3416.69	3.71
	0.1164	435.33	420.72	3.35
	0.2493	887.00	913.79	3.02
	0.3555	1288.62	1324.87	2.81
	0.4792	1814.38	1834.89	1.13
	0.5770	2267.58	2277.94	0.46
	0.6323	2568.05	2553.81	0.55
	0.7102	3064.85	2991.15	2.40
	0.7376	3255.26	3164.11	2.80
363.15	0.1144	462.78	450.45	2.66
	0.2484	1006.56	1017.98	1.13
	0.3548	1447.71	1500.79	3.67
	0.4776	2056.78	2102.75	2.24
	0.5765	2713.13	2637.63	2.78
	0.8576			
	0.9650			
	0.1196			
	0.2511			
	0.3572			

$$^a \delta p = (|p_{\text{exp}} - p_{\text{cal}}|/p_{\text{exp}}) \cdot (100 \%).$$

and γ_1 and x_1 represent the activity coefficient and the mole fraction of the refrigerant in the solution, respectively; the quantity $\exp[V_1^L(p - p_1^s)/RT]$ is the Poynting factor.

The saturation pressures of HFC-32 from (283.15 to 343.15) K were obtained using REFPROP.²³ The data were fitted with the extended Antoine equation.²⁴ The calculated values are shown in Table 2, in which p_{ref} is the saturation pressure obtained using REFPROP and $p_{\text{cal,sat}}$ is the saturation pressure obtained using the extended Antoine equation; the values of the parameters in the extended Antoine equation are shown in Table 3. From Table 2, it can be seen that the values calculated using the extended Antoine equation are in good agreement with the data from REFPROP.²³ The saturation pressures of HFC-32 at (353.15 and 363.15) K [which are beyond the critical temperature of HFC-32 (351.26 K)] were calculated using the extended Antoine equation.

The calculated p - T - x data are also listed in Table 1. The variation of the vapor pressure as a function of the mole fraction of HFC-32 (x_1) at different temperatures is shown in Figure 1.

Table 2. Saturation Pressures of HFC-32

T/K	$p_{\text{ref}}/\text{MPa}$	$p_{\text{cal,sat}}/\text{MPa}$	$\delta p_{\text{sat}}/\%a$
283.15	1.1069	1.1075	0.0541
293.15	1.4746	1.4751	0.0340
303.15	1.9275	1.9277	0.0112
313.15	2.4783	2.4779	0.0160
323.15	3.1412	3.1404	0.0257
333.15	3.9332	3.9338	0.0153
343.15	4.8768	4.8834	0.1361
353.15		6.0253	
363.15		7.4102	

$$^a \delta p_{\text{sat}} = (|p_{\text{ref}} - p_{\text{cal,sat}}|/p_{\text{ref}}) \cdot (100 \%)$$

Table 3. Parameters of the Extended Antoine Equation Derived by Fitting the Saturation Pressures Obtained Using REFPROP²³

parameter ^a	value
A	4.29712
B	833.1370
C	245.860
n	2.48212
E	61.006
F	-747.43

^a Extended Antoine equation: $\ln[p^s/(100 \text{ kPa})] = A - B/[C + (T/\text{K}) - 273.15] + 0.43429x^n + Ex^8 + Fx^{12}$, where $x = [(T/\text{K}) - (t_0/^\circ\text{C}) - 273.15]/(T_c/\text{K})$, in which $t_0 = -40^\circ\text{C}$.

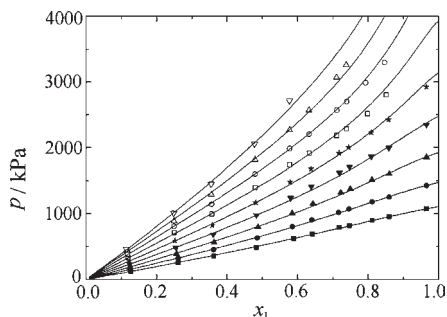
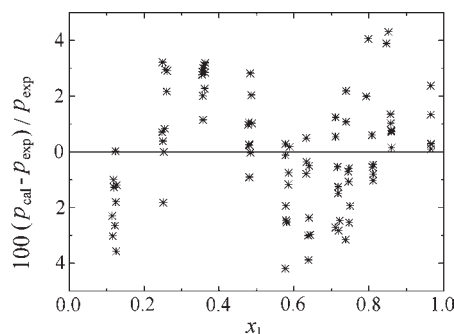
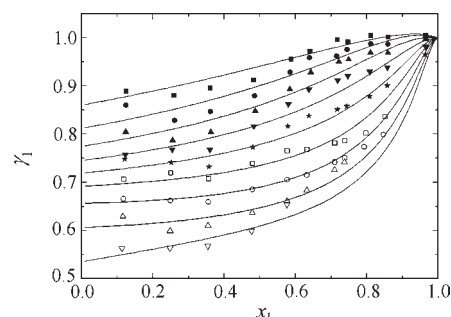
**Figure 1.** Solubility of HFC-32 in DMF as a function of temperature and pressure: ■, 283.15 K; ●, 293.15 K; ▲, 303.15 K; ▼, 313.15 K; ★, 323.15 K; □, 333.15 K; ○, 343.15 K; △, 353.15 K; ▽, 363.15 K. The solid lines were calculated using the NRTL model.

Figure 2 shows the relative pressure deviations of the experimental data from the values calculated using NRTL model, and Figure 3 gives the calculated activity coefficient of HFC-32 in DMF as a function of x_1 at different temperatures.

From Table 1 and Figures 1 to 3, it can be seen that the correlated results obtained using the NRTL model are in good agreement with the experimental data for the (HFC-32 + DMF) mixtures. The maximum deviation of the pressure was 4.24 %, and the average relative deviation (ARD) of the pressure was 1.65 %. Meanwhile, the results reveal that the mole fraction of HFC-32 in DMF at a specific temperature and pressure is higher than that predicted for an ideal solution obeying Raoult's law, that is, the mixture exhibits a negative deviation from Raoult's law. In addition, it can be seen that increasing the mass concentration of DMF

**Figure 2.** Relative deviations of the vapor pressure for (HFC-32 + DMF) binary mixtures at 283.15 K, 293.15 K, 303.15 K, 313.15 K, 323.15 K, 333.15 K, 343.15 K, 353.15 K, 363.15 K.**Figure 3.** Activity coefficient of HFC-32 in DMF as a function of mole fraction at various temperatures: ■, 283.15 K; ●, 293.15 K; ▲, 303.15 K; ▼, 313.15 K; ★, 323.15 K; □, 333.15 K; ○, 343.15 K; △, 353.15 K; ▽, 363.15 K. The solid lines were calculated using the NRTL model.**Table 4.** Parameters of the NRTL Model Derived by Fitting the Experimental Data

parameter	value
α	4
$\tau_{12}^{(0)}$	57443
$\tau_{12}^{(1)}$	-9780
$\tau_{21}^{(0)}$	30231
$\tau_{21}^{(1)}$	-5422
ARD/% ^a	1.65

^a The average relative deviation is defined as $\text{ARD} = (100 \%) \cdot \sum_{i=1}^N (|p_{\text{exp}} - p_{\text{cal}}|/p_{\text{exp}})_i / N$.

increases the negative deviation, and the main reason for this is that the weight errors are relatively big at high concentrations of DMF.

The values of the parameters $\tau_{12}^{(0)}$, $\tau_{12}^{(1)}$, $\tau_{21}^{(0)}$, $\tau_{21}^{(1)}$, and α are given in Table 4. As the interaction parameters τ_{12} and τ_{21} in the NRTL model were considered to be temperature-dependent in the calculation, the correlated results show that the NRTL model derived in this work can supply a good prediction over wide ranges of temperature and composition.

CONCLUSIONS

In this work, vapor–liquid equilibrium data for (HFC-32 + DMF) mixtures with various mass fractions over the temperature range (283.15 to 363.15) K were measured. During the experiment, there was no stratification or sediment generation in the liquid phase, and the color of the liquid phase in the equilibrium cell was

the same before and after the experiment. It has been shown that HFC-32 exhibits very good solubility characteristics with DMF as the solvent. Moreover, the NRTL model, including the effect of temperature on the interaction parameters, was used to correlate the experimental data; the ARD of the pressure was 1.65 %, and the maximum relative deviation of the pressure was 4.24 %. The predicted results show good agreement with the experimental data. In addition, the mixture exhibits a negative deviation from Raoult's law. This work shows that the HFC-32 and DMF might be a promising working pair for AHTs.

AUTHOR INFORMATION

Corresponding Author

*Tel: +86 571 8795 1738. Fax: +86 571 8795 2464. E-mail: wangqin@zju.edu.cn.

Funding Sources

This work was financially supported by the National Basic Research Program of China under Award 2010CB227304. The support of the Excellent Young Teachers Program of Zhejiang University (Zijin Program) is gratefully acknowledged.

REFERENCES

- (1) Kameyama, H. Heat pump technologies. *Chem. Eng.* **1998**, *62*, 718–721.
- (2) Eiseman, B. J. Why R22 should be favored for absorption refrigeration. *ASHRAE J.* **1959**, *12*, 45–50.
- (3) Bhaduri, S. C.; Varma, H. K. P – T – X behavior of refrigerant–absorbent pairs. *Int. J. Refrig.* **1985**, *8*, 172–175.
- (4) Agarwal, R. S.; Bapat, S. L. Solubility characteristics of R22–DMF refrigerant–absorption combination. *Int. J. Refrig.* **1985**, *8*, 70–74.
- (5) Bhaduri, S. C.; Verma, H. K. P – T – X behavior of R22 with five different absorptions. *Int. J. Refrig.* **1986**, *9*, 362–366.
- (6) Thieme, A.; Albright, L. F. Solubility of refrigerants 11, 21, and 22 in organic solvents containing a nitrogen atom and in mixtures of fluids. *ASHRAE J.* **1961**, *7*, 71–75.
- (7) Wang, J.; Zhen, D.; Fan, L.; Li, D. Vapor Pressure Measurement for the Water + 1,3-Dimethylimidazolium Chloride System and 2,2,2-Trifluoroethanol + 1-Ethyl-3-methylimidazolium Tetrafluoroborate System. *J. Chem. Eng. Data* **2010**, *55*, 2128–2132.
- (8) Jelinek, M.; Borde, I.; Yaron, I. Enthalpy–concentration diagram of the system R22–DIMETHYL FORMAMIDE and performance characteristics of refrigeration cycle operating with this system. *ASHRAE Trans.* **1978**, *84*, 60–67.
- (9) Bhaduri, S. C.; Verma, H. K. Heat of mixing of R22–absorbent mixture. *Int. J. Refrig.* **1988**, *11*, 181–185.
- (10) Fatuh, M.; Murthy, S. S. Comparison of R22–absorbent pairs for vapor absorption heat transformers based on P – T – X data. *Heat Recovery Syst. CHP* **1993**, *13*, 33–48.
- (11) Mark, O. M.; Eric, W. L.; Richard, T. J. Thermodynamic properties for the alternative refrigerants. *Int. J. Refrig.* **1998**, *21*, 322–338.
- (12) Borde, I.; Jelinek, M.; Daltrophe, N. C. Absorption system based on the refrigerant R134a. *Int. J. Refrig.* **1995**, *18*, 387–394.
- (13) McLinden, M. O.; Lemmon, E. W.; Jacobsen, R. T. Thermodynamic properties for the alternative refrigerants. *Refrig. 21st Century, ASHRAE/NIST Refrig. Conf., 3rd* **1997**, 10.
- (14) Tillner, R. R.; Yokozeki, A.; Sato, H.; Watanabe, K. *Thermodynamic Properties of Pure and Blended Hydrofluorocarbon (HFC) Refrigerants*; Japan Society of Refrigerating and Air Conditioning Engineers: Tokyo, 1998.
- (15) Calm, J. M.; Hourahan, G. C. Refrigerant Data Update. *Heat/Piping/Air Cond. Eng.* **2007**, *79*, 50–64.
- (16) Han, X.; Xu, Y. J.; Qiu, Y.; Min, X. W.; Gao, Z. J.; Chen, G. M. Experimental study on the cycle performance of refrigerant R32. *Refrig. Air Cond.* **2010**, *10*, 68–70.
- (17) Han, X.; Gao, Z. J.; Xu, Y. J.; Qiu, Y.; Min, X. W.; Wang, Q.; Chen, G. M. Isothermal vapor–liquid equilibrium data for the binary mixture difluoromethane (HFC-32) + ethyl fluoride (HFC-161) over a temperature range from 253.15 K to 303.15 K. *Fluid Phase Equilib.* **2010**, *299*, 116–121.
- (18) Lee, J.; Lee, J.; Kim, H. Vapor–liquid equilibria for HFC-32 containing systems. *Fluid Phase Equilib.* **1998**, *150–151*, 297–302.
- (19) Di Nicola, G.; Giuliani, G.; Polonara, F.; Stryjek, R. Blends of carbon dioxide and HFCs as working fluids for the low-temperature circuit in cascade refrigerating systems. *Int. J. Refrig.* **2005**, *28*, 130–140.
- (20) Qin, W.; Xu, Y. J.; Chen, X.; Gao, Z. J.; Han, S.; Han, X. H.; Chen, G. M. Experimental studies on a mixture of HFC-32/125/161 as an alternative refrigerant to HCFC-22 in the presence of polyol ester. *Fluid Phase Equilib.* **2010**, *293*, 110–117.
- (21) Renon, H.; Prausnitz, J. M. Local compositions in thermodynamic excess functions for liquid mixtures. *AIChE J.* **1968**, *14*, 135–144.
- (22) Han, X.; Zhu, Z. W.; Chen, F. S.; Xu, Y. J.; Gao, Z. J.; Chen, G. M. Solubility and Miscibility of the Mixture of (Ethyl Fluoride + Polyol Ester Oil). *J. Chem. Eng. Data* **2010**, *55*, 3200–3207.
- (23) McLinden, M.; Klein, S.; Lemmon, E.; Peskin, A. *NIST Thermodynamic and Transport Properties of Refrigerants and Refrigerant Mixtures Database (REFPROP)*, version 8.0; National Institute of Standards and Technology: Gaithersburg, MD, 2007.
- (24) Poling, B. E.; Prausnitz, J. M.; O'Connell, J. P. *The Properties of Gases and Liquids*; McGraw-Hill: New York, 2001.